Multimodal assessment of choroideremia patients defines pre-treatment characteristics

Immanuel P. Seitz · Ahmad Zhour · Susanne Kohl · Pablo Llavona · Tobias Peter · Barbara Wilhelm · Eberhart Zrenner · Marius Ueffing · Karl Ulrich Bartz-Schmidt · M. Dominik Fischer

Abstract

Purpose Choroideremia (CHM) is a X-chromosomal disorder leading to blindness by progressive degeneration of choroid, retinal pigment epithelium (RPE), and retinal neurons. A current clinical gene therapy trial (NCT01461213) showed promising safety and efficacy data in a carefully selected patient population. The present study was performed to shed light on pre-treatment characteristics of a larger cohort of CHM patients using a high resolution multi-modal approach.

Methods In a retrospective cross-sectional study, data from 58 eyes of 29 patients with clinically confirmed CHM were analysed including best-corrected visual acuity (BCVA), refractive error, spectral-domain optical coherence tomography (SD-OCT), fundus autofluorescence (FAF), perimetry, and tonometry. Residual retinal volume, area of residual RPE, and foveal thickness were quantified to further define natural disease progression and assess symmetry.

Results We evaluated 98 data points of BCVA [0.34±0.06 (logMAR); mean±95 % confidence interval], 80 of IOP (14.6±0.6 mmHg), and 98 of refraction (−2.16±1.08 spherical equivalent). Visual fields (n =76) demonstrated variable degrees of concentric constriction (54 % <10°, 25 % 10–30°, 21 % >30°). Mean residual RPE area on FAF (n =64) measured 8.47±1.91 mm^2 (range 0.30–38.5 mm^2), while mean neuroretinal volume (n =42) was found to be 1.76±0.12 mm^3. Age at examination was exponentially associated with BCVA, while logarithmic functions best described progressive loss of retinal area and volume. A high degree of left to right symmetry was found in all modalities with structural markers showing the best correlation (r^2_{area}=0.83; r^2_{volume}=0.75).

Conclusion Analysis of these widely available clinical data defines the natural disease characteristics of a relevant patient population eligible for gene therapeutic intervention. In the wake of preliminary reports on safety and efficacy of CHM gene therapy (NCT01461213), this multi-modal assessment of a cohort of CHM patients provides important evidence of the natural rate of disease progression and degree of symmetry between eyes.

I. P. Seitz · A. Zhour · E. Zrenner · K. U. Bartz-Schmidt · M. D. Fischer
University Eye Hospital, University of Tübingen, Tübingen, Germany

I. P. Seitz · S. Kohl · P. Llavona · E. Zrenner · M. Ueffing
Institute for Ophthalmic Research, University of Tübingen, Tübingen, Germany

T. Peter · B. Wilhelm
STZ Eyetrial, Centre for Ophthalmology, University of Tübingen, Tübingen, Germany

M. D. Fischer
Nuffield Laboratory of Ophthalmology, University of Oxford, Oxford, UK

M. D. Fischer
Oxford Eye Hospital, Oxford University Hospitals NHS Trust, Oxford, UK

M. D. Fischer (✉)
Merton College, University of Oxford, Oxford OX1 4JD, UK
e-mail: dominik.fischer@ndcn.ox.ac.uk

Introduction

Choroideremia (CHM) is a monogenic X-linked disorder causing progressive loss of vision. The clinical entity was recognised in the late 19th century, when a 32-year-old miller from the Puster valley in today's Italy (South Tyrol) presented in Prof. Mauthner's outpatient clinic in Innsbruck on 1 June

1871. The patient complained of nyctalopia and visual field constrictions, and showed all phenotypic hallmarks of the disease with centripetal atrophy of choroid, retinal pigment epithelium, and outer neuroretina [1].

Cremers and colleagues characterised the underlying genetic defect in the late 20th century [2–7]. In affected patients, the CHM locus (Xq21.2) may feature either pathogenic frameshift mutations or even larger deletions/insertions in *CHM*. Interestingly, CHM is uniquely coherent on a genetic level in that the vast majority of CHM is caused by null mutations, with complete absence of stable protein products [8]. *CHM* encodes for Rab escorting protein 1 (REP1), an ubiquitous enzyme important for intracellular vesicular transport [9]. Its homologue REP2 can compensate for *CHM* mutations in most other tissues, preventing a syndromic phenotype [10].

Despite more than 100 years of clinical observation, it is not entirely clear whether CHM primarily causes atrophy of the choroidal vasculature with secondary degeneration of retinal pigment epithelium (RPE) and photoreceptors, which rely on choroidal perfusion (as suggested first by Mauthner), or whether REP1 deficiency primarily causes death of RPE and photoreceptors with secondary atrophy of the choroid. Studies in mouse models of selective REP1 deficiency in photoreceptors, RPE, or both pointed to a potential cumulative pathogenic effect from both cell populations contributing to dysfunction and degeneration [11]. This prompted the use of a ubiquitous promoter for proof of concept studies, leading to a clinical safety study that would allow expression of the therapeutic coding sequence in all affected cell types [12].

Today, less than 25 years after the genetic cause was characterised, the first patients have been successfully treated in a pioneering clinical safety trial (NCT01461213) featuring a strategy of gene supplementation by adenovirus-associated viral vector delivery [13]. Preliminary data from this trial suggests that gene therapy is able to slow if not halt progression of degeneration in the treated eyes and possibly even reverse some previously under-recognised functional defects in areas not (yet) affected by the progressive atrophy associated with deficiency of REP1 [13]. While this study sets a milestone in the translational efforts in ophthalmology, it also highlights the importance to continuously review patients with hereditary retinal disorders (HRD) potentially suitable for future treatment options. Key questions during pre-treatment characterization of patients with choroideremia and HRDs in general concern: i) the precise spatial and temporal sequences of functional and structural defects in the natural disease progression to help determine windows of opportunity for intervention or maximal discriminatory power, ii) which parameters best serve as sensitive, specific, and robust outcome measures of therapeutic safety and efficacy, and furthermore, iii) how symmetric are those findings and is the fellow eye a suitable internal control?

This study was performed to address these questions by multi-modal clinical analysis of a cohort of patients with confirmed CHM. Only relatively recent data (recorded after January 2000) from 58 eyes (29 patients) were used in a retrospective cross-sectional study. We found evidence for exponential best fits for both functional and structural biomarkers over time, reflecting the centripetal disease progression on retinal level. Symmetry was high between right and left eyes and most robustly assessed by objectively quantifying the area of remaining retinal pigment epithelium in fundus autofluorescence recordings.

Materials and methods

Patients

This was a retrospective cross-sectional study in 58 eyes of 29 patients with clinically confirmed choroideremia (CHM), who were referred to the University Eye Hospital Tübingen between 2000 and 2014. The diagnosis of CHM was established based on a family history reflecting X-linked inheritance pattern and the characteristic fundus appearance. The study was performed in accordance with the tenets of the Declaration of Helsinki 1975 (1983 revision). Institutional review board approval was not required for this retrospective study as regulated by the data protection law of the state Baden–Württemberg, Germany.

Molecular assessment

Study participants were recruited over 20 years from the University Eye Hospital Tuebingen within the special day clinic for inherited retinal diseases. This and all our studies are performed according to the tenets of the Declaration of Helsinki, and all genetically tested participants gave written consent, approved by the local research and ethical review boards. Genomic DNA was extracted from peripheral blood samples using standard protocols. Genetic testing was performed in different laboratories with different research and diagnostic genetic setups. Recent testing in P15, P18, P20, and P23 followed the procedure published by Furgoch et al. [14]. All coding exons and flanking intron-exon boundaries of *CHM* were PCR-amplified with the primers described therein and sequenced. PCR fragments were purified by ExoSAP-IT treatment (USB, Cleveland, OH, USA), sequenced using Big Dye Termination chemistry (Applied Biosystems [ABI], Weiterstadt, Germany), and products separated on a DNA capillary sequencer (ABI 3100 genetic analyzer, Weiterstadt, Germany). Sequences were assembled and analysed with the SeqMan program (DNASTAR Lasergene Co., London, UK).

Clinical examinations

All subjects underwent slit-lamp examination, measurement of best-corrected distance visual acuity (D-BCVA) using Snellen charts, and visual field (VF) testing with semiautomated kinetic perimetry (SKP) using an Octopus 900 perimeter (Haag–Streit, Switzerland) or Goldmann perimetry as described previously [15, 16]. Briefly, the peripheral visual field boundary and blind spot were assessed using a size I4e target. A minimum of twelve vectors were assessed for the peripheral visual field inclusive of vectors offset from the vertical and horizontal meridia moving centripetally at 5°/sec (3°/sec for determination of the blind spot). Following assessment, the response points along each vector were joined to form the isopter for the I4e target. Average extend of this isopter in each eye was categorized as <10°, 10–30° or >30°.

Retinal imaging was performed on the same day after bilateral pupil dilation, and included spectral-domain optical coherence tomography (SD-OCT) and autofluorescence imaging (AF) using the Spectralis™ HRA+OCT platform (Heidelberg Engineering, Heidelberg, Germany) as described previously [17]. Pupillary mydriasis was induced using tropicamide eye drops 5 mg/ml (Mydriaticum Stulln, Pharma Stulln, Germany). For SD-OCT, multiple high-speed B-scans were recorded to assess central retinal architecture and quantify thickness of remaining neuro-retinal tissue. To improve signal to noise ratio (SNR), $n \geq 9$ scans were averaged for each B-scan recording, whereby SNR improved by the square root of n (i.e., SNR was at least tripled). Non-voluntary eye movements during averaging were corrected using the proprietary TruTrack™ function. AF data were recorded in the same session and settings (averaging and eye-tracking) using the same platform after switching from the SD-OCT mode to the HRA mode, which essentially records confocal scanning laser ophthalmoscopic (cSLO) images, after exciting retinal tissue at $\lambda = 488$ nm and introducing a barrier filter to collect light above $\lambda = 500$ nm [18]. For cSLO imaging, either the 30° or 55° optics of the Spectralis™ HRA+OCT platform was used depending on the extend of the residual central island. Proprietary software (Heidelberg Eye Explorer v1.6.4.0 and Spectralis Viewing Module 5.3.2.0) was used to quantify residual RPE islands and retinal thickness values (Fig. 1). For this, the border between the island of intact central retinal tissue and the atrophic periphery was determined by an experienced investigator (IPS) and reviewed by a fellow investigator (AZ), before area measurements produced by the proprietary software were recorded for statistical analysis. The border between the AF signal from remaining RPE and atrophic periphery was usually well defined and easy to delineate. In cases of any doubt, OCT scans recorded at the same time point were used to confirm location of the transitional zone between intact RPE/retina and atrophic area.
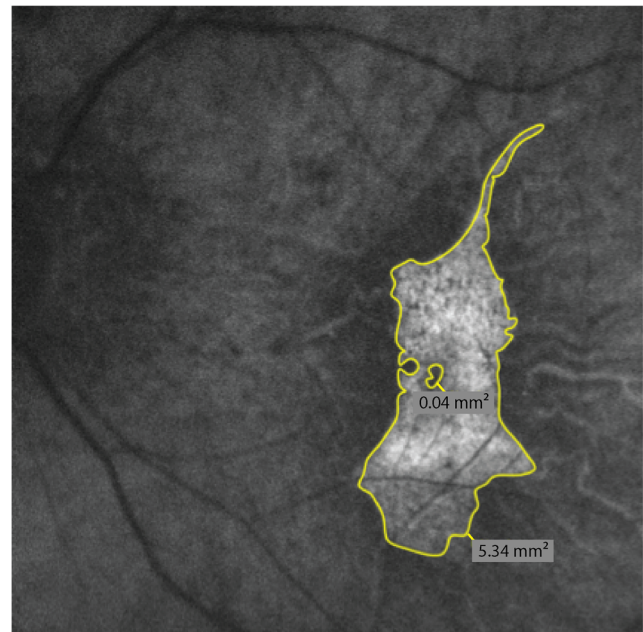

Fig. 1 Representative 30° autofluorescence recording from a patient with choroideremia (CHM). A *yellow line* was manually drawn around the area of remaining autofluoresecent islands of retinal pigment epithelium using the lasso tool of the proprietary software (Heidelberg Eye Explorer), which automatically reports the absolute area measurements. Note that any discontinuations (e.g., the small "hole" of 0.04 mm^2) within the island were subtracted from the overall area measurement

Statistical analysis

Bivariate correlation, *t*-tests and linear regression analyses were performed between modalities for cross-sectional progression analysis and between right and left eyes for symmetry analysis using Statistical Package for Social Sciences (SPSS) version 21 by IBM (SPSS Inc., Chicago, IL, USA) or Microsoft Excel version 14.1.0 (Microsoft, Redmond, Washington, USA), both for Macintosh OSX. Conversion of decimal BCVA data into logMAR was achieved by using the following formula: LogMAR = − Log (decimal acuity) [19]. Statistical significance was defined as $p < 0.05$.

Results

Overall cohort characteristics

Retrospective analysis of clinical data from the University Eye Hospital of Tübingen digital database revealed approximately 500 data points on visual function and retinal structure from 29 clinically confirmed CHM patients recorded between 2000 and 2014. Patients were either sporadic cases or presented with a family history consistent with X-linked inheritance. Clinical presentation was heterogeneous with respect to

disease severity. Age at examination ranged from 5 to 63 years. Mean and median age at examination were 42.5 and 48.0 years respectively.

Most patients reported about onset of nyctalopia in their teens, while central visual acuity typically remained largely unchanged until the fifth decade. All showed clear signs of peripheral and/or mid-peripheral atrophy of choroid, retinal pigment epithelium (RPE) and thinning of the retina due to photoreceptor loss, all in line with CHM.

Genetic test results

Genetic test results confirming the clinical diagnosis CHM were available for 25 patients at the time of publication (four patients did not consent to molecular diagnostics and/or did

not send blood samples). A list of the recorded mutations and their predicted effect is given in Table 1. The mutations observed in our patients most likely present null alleles, as they represent large deletions, nonsense mutations, or frame-shifting insertion/deletion mutations resulting in premature termination codons, all of which most likely undergo nonsense-mediated decay. This is in line with previous reports, which also show that the vast majority of CHM is caused by null mutations with complete absence of or instable protein products [8]. Novel mutations were observed in seven cases. The mutation spectrum comprises three nonsense mutations, two small frame-shifting deletions, three small frame-shifting duplications, two larger deletions covering exon 1 in patient 19 and exons 3–15 in the brothers 4 and 5, respectively, and two mutations resulting in missplicing.

Table 1 Results from molecular testing in patients with clinically confirmed choroideremia (CHM)

| Patient | Hemizygote mutations in *CHM* | | Comment |
	Nucleotide level	Protein level	
1	c.924 T>G	p.Tyr308*	van den Hurk et al. 2003
2	c.715C>T	p.Arg239*	Francis et al. 2005
3	c.124_133dup	p.Gly45Valfs*10	novel
4	deletion of exons 3-15	null	novel, brother of patient 5
5	deletion of exons 3-15	null	novel, brother of patient 4
6	c.1446delA	p.Gly483Glufs*15	van den Hurk et al. 1992
7	c.616dupA	p.T206NfsX17	brother of patient 8
8	c.616dupA	p.T206NfsX17	brother of patient 7
9	c.941-1G>T	splice defect / null	novel
10	c.924 T>G	p.Tyr308*	van den Hurk et al. 2003
11	n.a.	n.a.	no consent and/or no sample
12	n.a.	n.a.	no consent and/or no sample
13	c.314+10127 T>A	splice defect / null	van den Hurk et al. 2003, Hum Genet
14	n.a	n.a	no consent and/or no sample
15	c.1036G>T	p.Glu346*	novel
16	c.1531_1532delinsTCTTCT AAACAGCAT	p.Thr511Serfs*8	van den Hurk et al. 2003
17	c.924 T>G	p.Tyr308*	van den Hurk et al. 2003
18	c.1116_1117del	p.Leu374Valfs*43	novel
19	del Exon 1	null	confirmed; extent not defined
20	c.645del	p.Thr216Leufs*16	novel
21	c.715C>T	p.Arg239*	Francis et al. 2005
22	n.a.	n.a.	no consent and/or no sample
23	c.1476_1477dup	p.Cys493Tyrfs*6	novel
24	c.877C>T	p.R293X	van den Hurk et al. 2003
25	c.800delT	pT288Lfs*3	van den Hurk et al. 2003
26	deletion of exons 1-15	null	van den Hurk et al. 1992
27	c.653C>G	p.Ser218x	van den Hurk et al. 2003
28	c.757C>T	p.Arg253*	van den Hurk et al. 2003
29	c.116C>G	p.S39X	van den Hurk et al. 2003

Clinical outcome measures

Mean and 95 % confidence interval (CI) of 98 entries on logMAR visual acuity was 0.34±0.06. Intraocular pressure (n=80) was 14.6±0.6 mmHg, and refractive error (n =98) calculated as spherical equivalent was −2.16±1.08 overall. Visual fields (n= 6) demonstrated variable degrees of visual field loss, with half of the cohort (54 %) showing severe visual field constrictions (<10°), and two equal-sized groups (25 % and 21 %) with 10–30° and >30° remaining fields respectively. Mean residual RPE/neuroretinal area as quantified by fundus autofluorescence imaging (n =64) was 8.47±1.91 mm^2 (range 0.30–38.5 mm^2). Residual neuroretinal volume within the central macular area defined by the 3 mm ERTDS grid was 1.76±0.12 mm^3 (n=42).

Degree of intraindividual symmetry

In order to determine symmetry between right and left eyes in CHM patients at various disease stages, we firstly compared visual acuity measurements of the right and left eyes taken at the same time point and by the same experienced ophthalmologist. Linear regression analysis showed a good fit (r^2=0.64) indicating a rather symmetric development of visual acuity (Fig. 2a).

The objective quantification of residual area of fundus autofluorescence showed an even higher degree of symmetry (r^2=0.83) between right and left eyes of CHM patients (Fig. 2b). Using the 3-mm ETDRS grid, quantification of central retinal volume also showed a good degree of symmetry (r^2=0.75, Fig. 2c).

Disease progression and age

Rate of progression was tested in a cross-sectional fashion, correlating key biomarkers of visual function and retinal structure with age at examination in all patients. Central visual acuity and age at examination shows a relatively poor, exponential correlation (r^2=0.23) with good visual function until the 4th decade and subsequent rapid reduction of visual acuity as the degeneration encroaches the central retina (Fig. 3a).

Structural disease progression was determined directly and objectively by quantifying the residual area of intact fundus autofluorescence (Fig. 3b), which indicates metabolically active, viable retinal pigment epithelium. This biomarker consists of an area measurement in square mm, and bivariate correlation analysis with the linear measure age at examination indeed revealed a good logarithmic fit (r^2=0.67, Fig. 3). Analysis with volumetric data from the central 3 mm showed again only relatively poor correlation (r^2=0.25, Fig. 3c).
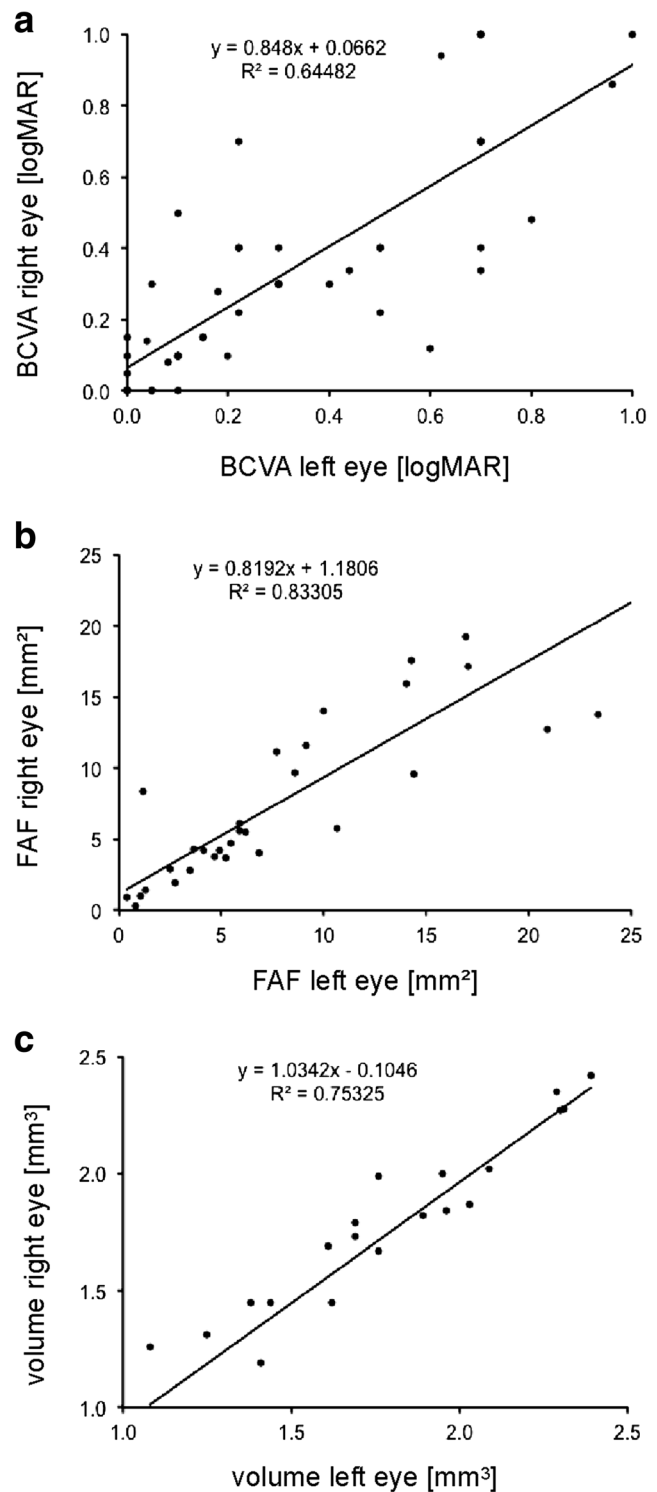

Fig. 2 Analysis of intraindividual symmetry in patients with choroideremia. **a** Best-corrected visual acuity (BCVA) as logarithm of the minimal angle of resolution (LogMAR) show high symmetry between right and left eyes (r^2=0.64). **b** Area of residual islands of intact fundus autofluorescence (FAF) was compared between right and left eyes (r^2=0.83). **c** Residual neuroretinal volume within the central 3 mm also correlated fairly well between eyes (r^2=0.75)
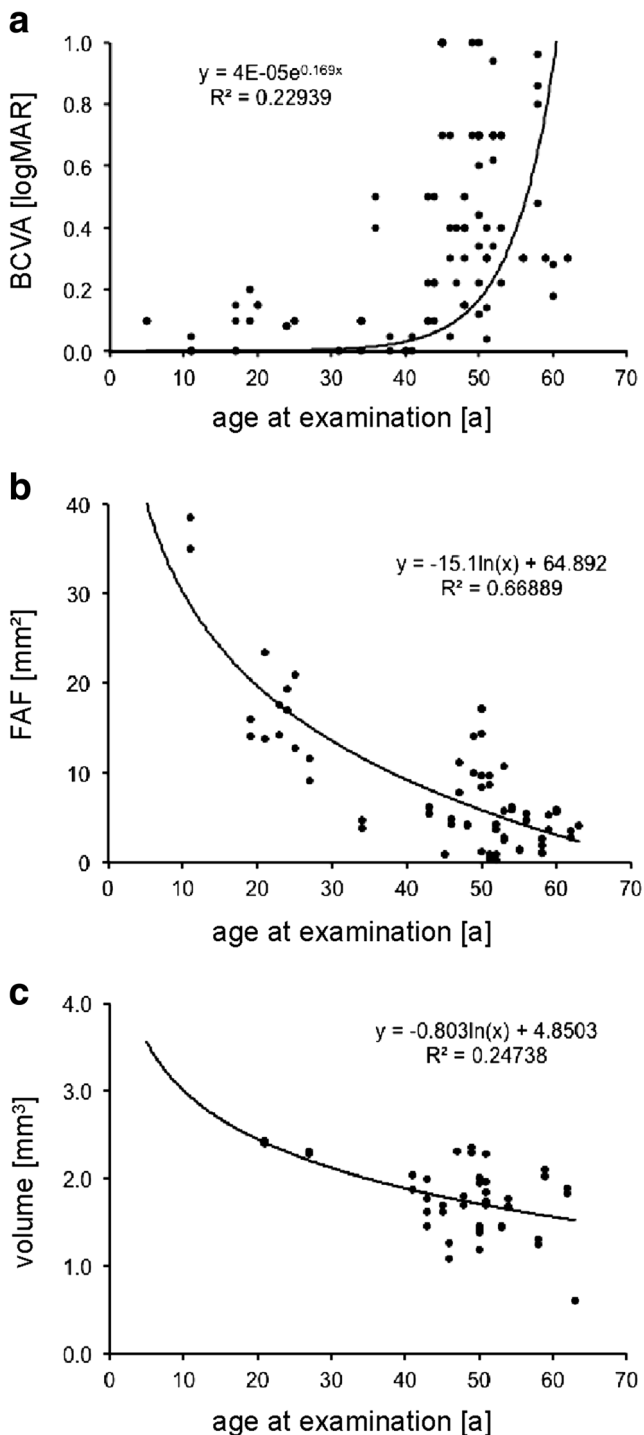
Fig. 3 Analysis of natural disease progression in patients with choroideremia. **a** Functional progression measured by best-corrected visual acuity (BCVA) in LogMAR (Logarithm of the minimal angle of resolution) vs age at examination describes an exponential function with visual acuity rapidly declining in later disease stages as the fovea becomes affected. Pearson correlation efficient $r^2 = 0.23$. **b** Structural markers of disease progression, such as size of the remaining island of intact fundus autofluorescence (FAF) measured in mm^2 best fit a logarithmic trend line ($r^2 = 0.69$) . **c** Volume measurements correlate with age at examination only marginally better then BCVA ($r^2 = 0.25$)

Discussion

The advent of gene therapeutic and other promising strategies for previously untreatable blinding disorders leads to a shift in management of patients with HRD. While previously considered of more or less purely academic interest, providing an accurate phenotypic and genetic characterisation now enables patients to potentially be selected for clinical trials aimed to help transfer the field of gene therapy into clinical reality.

Next to this, there are still a number of questions to be addressed by careful phenotyping, genotyping, and longitudinal follow up of patients with HRDs. As such, rate of progression is among the key questions, traditionally asked for prognostic reasons. With the advent of supplementation gene therapy and other potential strategies developed to slow or even stop progression, detailed knowledge of rate of progression can also provide information on the 'window of therapeutic opportunity' and help define end- and timepoints with high discriminatory power. In order to design interventional clinical trials, these data are essential in the process of defining eligibility of patients (e.g., when to treat), relevant efficacy measures, and time schedules for study visits during follow-up. Here, knowledge on the rate of natural disease progression and degree of symmetry becomes paramount.

This study contributes to this knowledge in CHM patients by testing the relationship of key functional and structural biomarkers with age of the respective patient and assessing symmetry of these biomarkers between the right and left eye of CHM patients. To the best of our knowledge, there is currently no quantitative analysis published on the intra-individual symmetry of important clinical parameters, which may serve as surrogate markers for therapeutic efficacy after unilateral intervention in a clinical trial setting. Given that (for example) additive gene therapy is applied locally and to the benefit of the treated eye only, knowledge of the degree of symmetry between eyes is of strategic value. Analysis of data between right and left eyes showed high degrees of symmetry, with data on area measurements of fundus autofluorescence outperforming residual retinal volume and the psychophysical measurement of visual acuity showing the least symmetry (FAF: $r^2 = 0.83$; volume: $r^2 = 0.75$; BCVA: $r^2 = 0.64$). This may simply reflect the higher level of integration present in psychophysical measures (optical media, cognition, et cetera) compared to simple bio-morphological quantification, which is bound to introduce more variability in the outcome measure.

In terms of visual acuity and age at examination, our study showed a poor linear correlation ($r^2 = 0.16$) and only slightly better fit for an exponential trend line ($r^2 = 0.23$). This pattern of VA deterioration has been described previously, and precisely reflects the non-uniform distribution of resolving power in the retina, with the fovea being the most important contributor to Snellen visual acuity and the last to be affected in the

centripetal course of degeneration. Rate of progression was 0.0103 logMAR per year in the linear model, which is very similar to what Coussa et al. reported (0.0072) in a slightly younger cohort (36±17.7) [20]. Roberts et al. found an annual loss of 0.09 logMAR in a retrospective longitudinal study with data sets from different tertiary referral centres [21] Interestingly, Coussa et al. reported a higher annual loss of visual acuity (0.06±0.08 log MAR) for patients in the >50 age group, indicating a more rapid vision loss in older patients. This supports our observation of an exponential, rather than linear decline of VA with age. Thus, the above linear predictions probably overestimate progression until ca. age 40, and underestimate the development beyond, and differences in reported functional progression may stem from differences in cohort characteristics such as age. The improvement of fit with choosing an exponential trend line reflects the known clinical course of CHM patients, maintaining a good visual function until approximately the 5th decade of life, with a subsequent rapid reduction of visual acuity as the degeneration starts to affect the fovea. Importantly, fundus autofluorescence provided a structural biomarker with a markedly closer fit (r^2=0.67) with regard to the relationship to age at examination, possibly benefiting from the lack of increasing variability, which affect psychophysical outcome measures to a greater extent in advanced disease stages [22].

These data suggest that treatment at a later stage of the disease would give the best discriminatory power between treated and untreated eyes, as the exponential curve is steepest due to rapid loss of remaining retinal tissue and disproportionally large impact on visual acuity. While this is scientifically plausible, it poses an ethical dilemma for the physician, who retains a safe and potentially efficacious treatment from the patient with certain progression to blindness. The study design of the phase II trial for Leber's congenital amaurosis (LCA) in Philadelphia addresses this problem by allowing the treatment of the second eye after a certain time period of following the natural disease progression (personal communication Dr. Bennett).

This compromise follows the reasoning that the untreated fellow eye is an appropriate internal control in LCA patients, which is likewise true for CHM as confirmed by this study. More specifically, our data indicate that while symmetry is high for both structural and functional biomarkers, quantitative assessment of residual RPE area might be a superior outcome measure compared to visual acuity from a scientific point of view. Firstly, it is easier to mask readout, as quantification can be performed without patient interaction by experts outside the trial unit (e.g., reading centre). In contrast, masking strategies for BCVA assessment will always be incomplete. Even if the examiner recording the BCVA was successfully masked for the treatment, the patient would not be. Therefore, one has to assume confounding effects by motivation and expectation that may influence efficacy results.

There is ample evidence with regard to the increased variability of BCVA results in patients with low visual acuity [22]. Alas, increasing the numbers of successfully identified ETDRS letters remains the gold standard treatment goal — especially in the pursuit of gaining market approval and complying with the checklists of regulatory agencies.

It will remain an important challenge for clinicians and scientists to provide a solid body of evidence supporting the argument that interventions such as gene therapy are efficacious if they stop further degeneration, rather than leading to an improvement of visual acuity. This even more so in disorders similar to CHM, where patients maintain very good central visual acuity until the very end of the disease course. We argue that preventing the degeneration at an earlier time point might be the more viable approach, rather than waiting for foveal involvement, when gene therapy has only limited remaining therapeutic potential, as most target cells have already undergone degeneration.

References

1. Mauthner L (1872) Ein Fall von Chorioideremie. Bericht des Naturwissenschaftlich-Medizinischen Vereins Innsbruck:191–197

2. Cremers FP, Brunsmann F, van de Pol TJ, Pawlowitzki IH, Paulsen K, Wieringa B, Ropers HH (1987) Deletion of the DXS165 locus in patients with classical choroideremia. Clin Genet 32:421–423

3. Cremers FP, van de Pol DJ, Diergaarde PJ, Wieringa B, Nussbaum RL, Schwartz M, Ropers HH (1989) Physical fine mapping of the choroideremia locus using Xq21 deletions associated with complex syndromes. Genomics 4:41–46

4. Cremers FP, van de Pol DJ, Wieringa B, Collins FS, Sankila EM, Siu VM, Flintoff WF, Brunsmann F, Blonden LA, Ropers HH (1989) Chromosomal jumping from the DXS165 locus allows molecular characterization of four microdeletions and a de novo chromosome X/13 translocation associated with choroideremia. Proc Natl Acad Sci U S A 86:7510–7514

5. Cremers FP, Sankila EM, Brunsmann F, Jay M, Jay B, Wright A, Pinckers AJ, Schwartz M, van de Pol DJ, Wieringa B et al (1990)

Deletions in patients with classical choroideremia vary in size from 45 kb to several megabases. Am J Hum Genet 47:622–628

6. Cremers FP, Molloy CM, van de Pol DJ, van den Hurk JA, Bach I, Geurts van Kessel AH, Ropers HH (1992) An autosomal homologue of the choroideremia gene colocalizes with the Usher syndrome type II locus on the distal part of chromosome 1q. Hum Mol Genet 1:71–75

7. Cremers FP, Armstrong SA, Seabra MC, Brown MS, Goldstein JL (1994) REP-2, a Rab escort protein encoded by the choroideremia-like gene. J Biol Chem 269:2111–2117

8. Coussa RG, Traboulsi EI (2012) Choroideremia: a review of general findings and pathogenesis. Ophthalmic Genet 33:57–65

9. Rak A, Pylypenko O, Niculae A, Pyatkov K, Goody RS, Alexandrov K (2004) Structure of the Rab7:REP-1 complex: insights into the mechanism of Rab prenylation and choroideremia disease. Cell 117:749–760

10. Moosajee M, Ramsden SC, Black GC, Seabra MC, Webster AR (2014) Clinical utility gene card for: choroideremia. Eur J Hum Genet 22(4)

11. Wavre-Shapton ST, Tolmachova T, Lopes da Silva M, Futter CE, Seabra MC (2013) Conditional ablation of the choroideremia gene causes age-related changes in mouse retinal pigment epithelium. PLoS One 8:e57769

12. Tolmachova T, Tolmachov OE, Barnard AR, de Silva SR, Lipinski DM, Walker NJ, Maclaren RE, Seabra MC (2013) Functional expression of Rab escort protein 1 following AAV2-mediated gene delivery in the retina of choroideremia mice and human cells ex vivo. J Mol Med 91:825–837

13. MacLaren RE, Groppe M, Barnard AR, Cottriall CL, Tolmachova T, Seymour L, Clark KR, During MJ, Cremers FP, Black GC, Lotery AJ, Downes SM, Webster AR, Seabra MC (2014) Retinal gene therapy in patients with choroideremia: initial findings from a phase 1/2 clinical trial. Lancet 383:1129–1137

14. Furgoch MJ, Mewes-Ares J, Radziwon A, Macdonald IM (2014) Molecular genetic diagnostic techniques in choroideremia. Mol Vis 20:535–544

15. Fischer MD, Fleischhauer JC, Gillies MC, Sutter FK, Helbig H, Barthelmes D (2008) A new method to monitor visual field defects caused by photoreceptor degeneration by quantitative optical coherence tomography. Invest Ophthalmol Vis Sci 49:3617–3621

16. Wiethoff S, Zhour A, Schols L, Fischer MD (2012) Retinal nerve fibre layer loss in hereditary spastic paraplegias is restricted to complex phenotypes. BMC Neurol 12:143

17. Fischer MD, Willmann G, Schatz A, Schommer K, Zhour A, Zrenner E, Bartz-Schmidt KU, Gekeler F (2012) Structural and functional changes of the human macula during acute exposure to high altitude. PLoS One 7:e36155

18. Bellmann C, Rubin GS, Kabanarou SA, Bird AC, Fitzke FW (2003) Fundus autofluorescence imaging compared with different confocal scanning laser ophthalmoscopes. Br J Ophthalmol 87:1381–1386

19. Holladay JT (1997) Proper method for calculating average visual acuity. J Refract Surg 13(4):388–391

20. Coussa RG, Kim J, Traboulsi EI (2012) Choroideremia: effect of age on visual acuity in patients and female carriers. Ophthalmic Genet 33:66–73

21. Roberts MF, Fishman GA, Roberts DK, Heckenlively JR, Weleber RG, Anderson RJ, Grover S (2002) Retrospective, longitudinal, and cross sectional study of visual acuity impairment in choroideraemia. Br J Ophthalmol 86:658–662

22. Bittner AK (2011) Variability in vision and photopsias in retinitis pigmentosa are related to disease severity and psychosocial factors. Dissertation. The Johns Hopkins University